

1 **Refined mapping of tree cover at fine-scale using time-series**
2 **Planet-NICFI and Sentinel-1 imagery for Southeast Asia (2016-**
3 **2021)**

4 Feng Yang^a, Zhenzhong Zeng^{a,*}

5 ^a School of Environmental Science and Engineering, Southern University of Science and Technology,
6 Shenzhen 518055, China

7

8

9 * Correspondence to: zengzz@sustech.edu.cn (Zhenzhong Zeng)

10 Mailing Address:

11 College of Engineering N808

12 Southern University of Science and Technology

13 Shenzhen, China

14

15

16

17 The manuscript for *Earth System Science Data*

18 July 31, 2023

19

20 **Abstract:**

21 High-resolution mapping of tree cover is indispensable for effectively addressing tropical forest carbon loss,
22 climate warming, biodiversity conservation, and sustainable development. However, the availability of
23 precise high-resolution tree cover map products remains inadequate due to the inherent limitations of
24 mapping techniques utilizing medium-to-coarse resolution satellite imagery, such as Landsat and Sentinel-2
25 imagery. In this study, we have generated an annual tree cover map product at a resolution of 4.77 m for
26 Southeast Asia (SEA) for the years 2016-2021 by integrating Planet-Norway's International Climate &
27 Forests Initiative (NICFI) imagery and Sentinel-1 Synthetic Aperture Radar data. ~~We~~ have also collected
28 annual [tree cover/non-tree cover](#) samples to assess the accuracy of our Planet-NICFI tree cover map product.
29 The results show that our Planet-NICFI tree cover map product during 2016-2021 achieve high accuracy,
30 with an overall accuracy of $\geq 0.867 \pm 0.017$ and a mean F1 score of 0.921, respectively. Furthermore, our tree
31 cover map product exhibits high temporal consistency from 2016 to 2021. Compared to existing map products
32 (FROM-GLC10, ESA WorldCover 2020 and 2021), our tree cover map product exhibits better performance,
33 both statistically and visually. Yet, the imagery obtained from Planet-NICFI performs less in mapping tree
34 cover in areas with diverse vegetation or complex landscapes due to insufficient spectral information.
35 Nevertheless, we highlight the capability of Planet-NICFI datasets in providing quick and fine-scale tree
36 cover mapping to a large extent. The consistent characterization of tree cover dynamics in SEA's tropical
37 forests can be further applied in various disciplines. ~~Our data~~ from 2016 to 2021 at a 4.77 m resolution are
38 publicly available at <https://cstr.cn/31253.11.sciencedb.07173> (Yang and Zeng, 2023).

Deleted: we

Deleted: The annual Planet-NICFI V1.0

Deleted: tree cover map products

40 **1 Introduction**

41 Forests and tree-based systems outside forests play a crucial role in land-based carbon emissions or removals,

45 making them essential for supporting and monitoring the implementation of the Reducing Emissions from
46 Deforestation and Forest Degradation (REDD+) and other land-based activities under the Paris Agreement
47 (Skea et al., 2022; CoP26, 2021; FAO, 2020). However, current forest cover map products exhibit significant
48 errors in accurately estimating forest area and change, particularly in areas such as trees outside forests and
49 forest edge landscapes (Mugabowindekwe et al., 2023; Reiner et al., 2022; Brandt et al., 2020). As a result,
50 there is a growing demand for timely, high-quality, and high-resolution tree cover products to accurately
51 capture the dynamics and changes in tree cover.

52

53 Many tree cover map products have been developed at medium-to-coarse resolutions (10-500 m), such as
54 Finer Resolution Observation and Monitoring of Global Land Cover 10 m (FROM-GLC10; Gong et al.,
55 2019), Environmental Systems Research Institute (ESRI) Land Cover (2017-2021) (Karra et al., 2021),
56 European Space Agency (ESA) WorldCover 2020 and 2021 (Zanaga et al., 2022; Zanaga et al., 2021), GFC
57 (Hansen et al., 2013), Globeland30 (Chen et al., 2015), Copernicus Global Land Service (CGLS) Land Cover
58 (Buchhorn et al., 2020), ESA Climate Change Initiative (CCI)(ESA, 2017) and the National Aeronautics and
59 Space Administration (NASA) MCD12Q1 (Friedl and Sulla-Menashe, 2019). However, accurate high-
60 resolution tree cover map products at continental-to-global scales are still lacking due to mapping through
61 medium-to-coarse resolution imagery (Zanaga et al., 2021; Hansen et al., 2010). Consequently, some
62 uncertainties occur in acquiring global tree inventories and monitoring forest disturbances (deforestation and
63 forest degradation). This is mainly due to isolated trees or long narrow forest cover removal (Reiner et al.,
64 2022; Wagner et al., 2022; Sexton et al., 2016; Hammer et al., 2014; Hsieh et al., 2001).

65

66 Only recently have two tree cover map products at <4.77 m from preprints been produced over Africa and

67 the state of Mato Grosso in Brazil using Planet-Norway's International Climate & Forests Initiative (NICFI)
68 imagery based on deep learning (Wagner et al., 2023; Reiner et al., 2022). However, these two maps have
69 only limited temporal or spatial coverage that occurred. Since the early 21st century, agricultural expansion
70 has created a new wave of drastic land use/land cover changes in Southeast Asia (SEA), leading the region
71 to be one of the most deforested regions worldwide (Zeng et al., 2018a; Zeng et al., 2018b; Achard et al.,
72 2014). Average elevations and slopes of forest loss sites have significantly increased in SEA, particularly in
73 the 2010s, geometrically irregular upland land use sites commonly occur (Velasco et al., 2022; Feng et al.,
74 2021). However, existing tree cover map products have underestimated deforestation (25-116%) and upland
75 agricultural expansion rates (9-113%), especially on the topographic boundaries in SEA (Zeng et al., 2018a).
76 Thus, fine-resolution tree cover map products in SEA, with high spatial resolution and longer consistent time
77 series, are urgently needed to accurately monitor tree cover loss and related illegal deforestation. In addition,
78 combining high-resolution optical imagery and Synthetic Aperture Radar (SAR) data (Sentinel-1) to produce
79 large-area tree cover map products is still in its early stage (Zanaga et al., 2022; Karra et al., 2021; Zanaga et
80 al., 2021; Buchhorn et al., 2020; Hansen et al., 2010).

81
82 Concurrently, advances in large-scale cloud computing (e.g., Google Earth Engine, GEE; Gorelick et al.,
83 2017) and available high-resolution satellite imagery (Roy et al., 2021) can facilitate the development of
84 high-resolution and longer time-series tree cover map products at continental-to-global scales. In this paper,
85 we generated state-of-the-art fine-scale open-source tree cover maps for SEA during 2016-2021 using Planet-
86 NICFI imagery, Sentinel-1 SAR data, and the random forest (RF) method from a previous study (Yang et al.,
87 2023). This dataset allows for extensive assessments of forest dynamics change, such as deforestation, forest
88 degradation, and reforestation. In addition, our dataset can monitor trees outside forests and long narrow

89 forest cover removal, thus improving the accuracy of automated continental tree inventories, which helps
90 optimize REDD+ under the Paris Agreement.

91

92 **2 Materials and method**

93 **2.1 Satellite imagery**

94 We utilized Planet-NICFI and Sentinel-1 imagery for the years 2016-2021 to generate a time series tree cover
95 map product for SEA. The Planet-NICFI program provides high-resolution (4.77 m per pixel) optical
96 PlanetScope surface reflectance mosaics specifically designed for the tropics. These mosaics offer accurate
97 and reliable spatial data with minimized effects from atmosphere and sensor characteristics, making them an
98 ideal 'ground truth' representation (Planet Team, 2017). The mosaics cover the best imagery to represent every
99 part of the coverage area during leaf-on periods from June to November based on cloud cover and acutance
100 (image sharpness). The Planet-NICFI imageries consist of four bands: red, green, blue, and near-infrared, and
101 cover a time period from 2015 to 2020 at bi-annual resolution for the archive, and from 2020 to 2023 at
102 monthly resolution for monitoring purposes. We accessed and utilized these products in the GEE platform by
103 authorizing our NICFI account to the GEE account.

104

105 We utilized Sentinel-1 on the GEE platform, specifically the 10 m resolution dual-polarization Ground Range
106 Detected (GRD) scenes (VV + VH). We chose Sentinel-1 SAR imagery to correct cases of overestimation
107 caused by confusion with herbaceous vegetation, or underestimation due to optical satellite observations
108 omitting deciduous or semi-deciduous characteristics (Shimada et al., 2014). The SAR imagery, available
109 every 12 days for a single satellite or 6 days for a dual-satellite constellation from October 2014 to the present,
110 was pre-processed with the Sentinel-1 Toolbox for thermal noise removal, radiometric calibration, and terrain

111 correction.

112

113 2.2 Validation dataset collection

114 We collected time series validation datasets to comprehensively assess the tree cover map product during
115 2016-2021, except for 2019 as it has been provided by Yang et al. (2023). Our mapping approach has been
116 comprehensively assessed after being developed in 2019 (Yang et al., 2023). However, despite the
117 advancements in the Land Cover Land Use Change (LCLUC) community, a notable gap remains the absence
118 of publicly available high-resolution (e.g., <10 m) tree cover/non-tree cover labels. The existing coarse-
119 resolution labels for tree cover/non-tree cover can introduce considerable uncertainties when evaluating high-
120 resolution tree cover maps. As a result, our ability to delve deeper into the accuracy of time-series tree cover
121 map datasets was hindered.

122

123 Following the methodology established by Yang et al. (2023), we undertook a rigorous process to generate a
124 robust validation dataset for our study. Firstly, we randomly generated 1,515 points to ensure a representative
125 sample of collected visual data, as illustrated in Fig. 1. Next, to classify these points as trees or non-trees, we
126 enlisted four human interpreters and employed Planet Explorer within QGIS. Our approach involved visually
127 identifying tree cover/non-tree cover pixels in the true color composite of Planet-NICFI imagery where the
128 points were located. To ensure accuracy, we superimposed the 10 m tree height data, previously developed
129 by Lang et al. (2022), onto the Planet-NICFI imagery. This step ensured that the labels adhered to the specified
130 tree height criteria (i.e., >5 m). Subsequently, we thoroughly evaluated and refined the labels using Google
131 Earth. To make time series tree cover/non-tree cover labels, we maintained the geographic location of the
132 1,515 points and changed the year of the Planet-NICFI imagery. The resulting labels encompassed data from

Deleted: other

Deleted: (Lang et al., 2022)

Deleted: tested

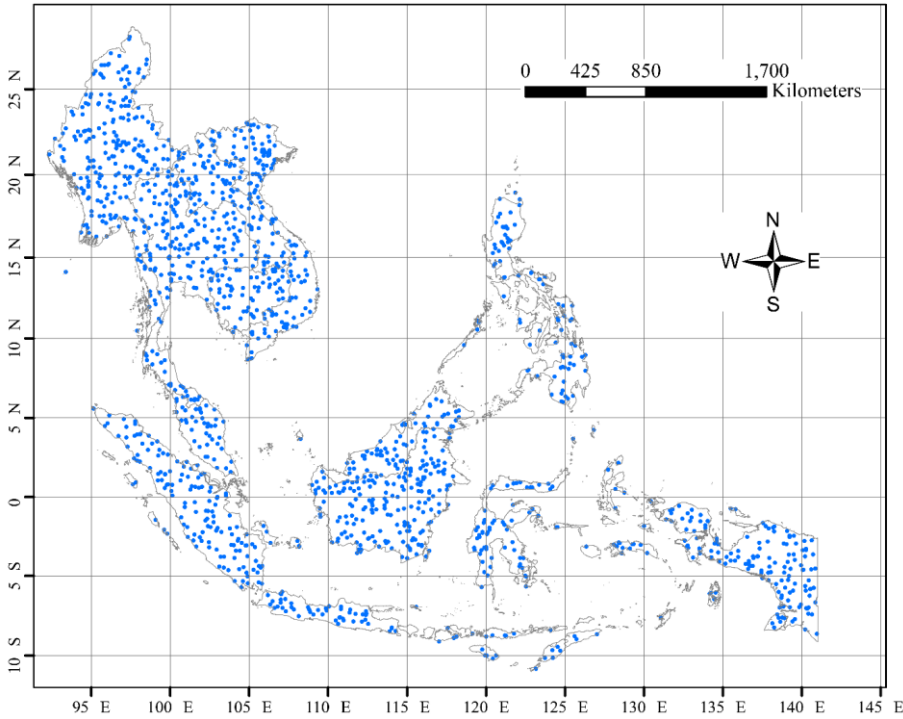
Deleted: However, we were unable to obtain suitable validation datasets to investigate the accuracy of our time-series tree cover datasets because existing samples mainly have coarse resolutions (e.g., ≥ 10 m)

Deleted: This can cause significant uncertainties in assessing high-resolution tree cover maps.

Deleted: Thus, following Yang et al. (2023), we randomly generated 1,515 points to ensure the representativeness of collected visual samples (Fig. 1)

145 the years 2016, 2017, 2018, 2020, and 2021. Comprehensive information about the validation dataset can be
 146 found in Table 1.

Deleted: Then, these points were labeled these points as forests or non-forests by four human interpreters using Planet Explorer of QGIS. During labeling, we fixed the location of the 1,515 points and changed the year of the Planet-NICFI imagery. The labels included 2016, 2017, 2018, 2020, and 2021. In addition, we overlapped the 10 m tree height data of Lang et al. (2022) over the Planet-NICFI imagery to ensure that the labels met the tree height criteria (i.e., ≥ 5 m). Detailed information on the validation dataset is listed in Table 1.



147 **Figure 1** Spatial distribution of randomly generated 1,515 validation dataset points.
 148

149 **Table 1** Information of the mapped validation dataset for evaluating the generated tree cover map product.
 150

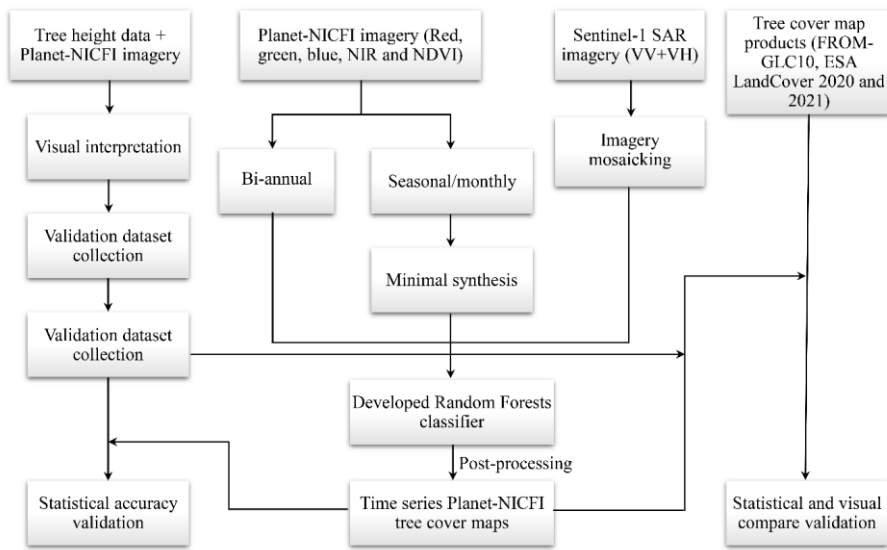
| Period | Count of sample points | | |
|--------|------------------------|---------------------------|-------|
| | Tree cover | Non-free cover | Total |
| 2016 | 1,086 | 429 | 1,515 |
| 2017 | 1,026 | 489 | 1,515 |
| 2018 | 977 | 538 | 1,515 |
| 2020 | 1,093 | 422 | 1,515 |
| 2021 | 952 | 563 | 1,515 |

Deleted: Forest
Deleted: forest
Deleted: 126
Deleted: 389

151

166 **2.3 Method**

167 We integrated Planet-NICFI and Sentinel-1 SAR imagery to generate a high-resolution (4.77 m) annual tree
168 cover map product for SEA covering the years 2015-2021. Our framework involved several key steps,
169 including defining mapped objects, preprocessing of imagery, and generation of time-series tree cover map
170 product. The detailed workflow is illustrated in Fig. 2.



171 **Figure 2** Workflow of generating tree cover products for 2016-2021, including imagery preprocessing,
172 generation of tree cover map product, and accuracy validation.
173

174

175 2.3.1 Definition of mapped tree cover

176 Traditionally, forests are considered to meet specific criteria (tree cover and height). The Food and Agriculture
177 Organization (FAO) of the United Nations defines forests as land spanning more than 0.5 hectares with trees
178 higher than 5 m and a canopy cover above 10% (FAO, 2020). According to the United Nations Framework
179 Convention on Climate Change (UNFCCC), forests are defined as areas with a minimum canopy cover of
180 10-30%, minimum tree height of 2-5 m, and a minimum area of 0.1 ha (Parker et al., 2008).

Deleted: objects

Deleted: For example, t

183
184 In this study, tree cover is defined as any geographic area dominated by trees without a percentage of tree
185 coverage at the pixel level (Zanaga et al., 2020; Hansen et al., 2013). This is attributed to the fact that the
186 resolution of the Planet pixel (4.77 m) is closer to the size of trees in tropical areas. Next, we utilized Planet-
187 NICFI imagery to generate only a prototype tree cover map with a resolution of 4.77 m and trees higher than
188 5 m. Our tree cover map product serves as baseline data for forest cover analysis. Upon further development
189 of the map to include trees higher than 5/2-5 m, it can be utilized for deriving forest maps for various functions,
190 such as those provided by FAO and UNFCCC.

191
192 2.3.2 Preprocessing of imagery

193 We utilized the GEE platform to preprocess Planet-NICFI imagery and Sentinel-1 SAR data for generating
194 tree cover maps for the years 2016-2021 (Fig. 2). Specifically, following the methodology of Yang et al.
195 (2023), we first employed the ee.ImageCollection.mosaic() function to merge and assemble overlapping
196 Sentinel-1 SAR data over the specified time period into a seamless, continuous imagery. Subsequently, we
197 performed bilinear resampling on the SAR imagery, specifically the VV and VH bands, to match the spatial
198 resolution of Planet-NICFI imagery, with a spatial resolution of 4.77 m.

Deleted: to

Deleted: generate

Deleted: Following

Deleted: obtain a high-resolution tree cover map

199
200 Planet-NICFI offers imagery at two different temporal frequencies spanning from 2016 to 2021. This includes
201 semi-annual imagery from 2016 to 2019 and monthly data from 2020 to 2021. To create a coherent and
202 consistent dataset for 2020 and 2021, we synthesized the selected time window of monthly imagery into
203 single imagery for each band, namely red, green, blue, and near-infrared bands. Specifically, we utilized the
204 ee.ImageCollection.min() function on each monthly imagery to extract the minimum monthly imagery, which

209 was then used to generate the second semi-annual imagery for 2020 and 2021. This approach was employed
210 to minimize the impact of cloud pollution on Planet-NICFI imagery (Oishi et al, 2018).

211

212 2.3.3 Generation of time-series tree cover map product

213 In addition to applying the RF approach in our tree cover mapping (Yang et al., 2023), RF-based methods
214 have been widely employed to develop global LCLUC products and show good performance (Zanaga et al.,
215 2022; Zanaga et al., 2021; Buchhorn et al., 2020). To acquire the time-series tree cover map dataset, our
216 methodology involved a two-step process. Initially, we integrated our custom RF approach, implemented on
217 Google Earth Engine (GEE), with a cloud-based machine learning platform. This combination enabled us to
218 obtain semi-annual Planet-NICFI and Sentinel-1 imageries spanning the years 2016 to 2021, as illustrated in
219 Fig. 2. Following data acquisition, we performed several post-processing steps to generate accurate tree cover
220 map product for the SEA region. These steps included downloading the acquired data from the cloud platform
221 to a local location, conducting mosaic operations, clipping relevant areas, applying projection transformations,
222 and performing correlation statistics. By employing this comprehensive approach, we successfully produced
223 a high-resolution tree cover map product,

Deleted: land cover and land use (LCLU)

224

225 2.3.4 Statistical accuracy assessment

226 We used two methods to assess the statistical accuracy of our tree cover map product. The generated tree
227 cover map product is compared pixel by pixel with the tree cover/non-tree cover labels. We then obtained a
228 confusion matrix, including true tree cover (TP), true non-tree cover (TN), false tree cover (FP), and false
229 non-tree cover (FN). These four values are used to calculate the user's accuracy, producer's accuracy, and
230 overall accuracy at a 95% confidence level (Olofsson et al., 2014) and the F1 score based on Eqs. (1)-(4),
231 respectively.

Deleted: To obtain our time-series tree cover datasets, we combined our RF approach using GEE with a cloud machine learning platform to obtain semi-annual Planet-NICFI and Sentinel-1 imageries for years 2016-2021 (Fig. 2). We then conducted various postprocessing to generate tree cover products for SEA, including downloading from a cloud platform to a local location, mosaic, clip, projection, and correlation statistics.

Deleted: We first used the confusion matrix

$$\text{User's accuracy (UA)} = \frac{TP}{TP + FP} \quad (1)$$

$$\text{Producer's accuracy (PA)} = \frac{TP}{TP + FN} \quad (2)$$

$$\text{Overall accuracy} = \frac{TP + TN}{TP + TN + FP + FN} \quad (3)$$

$$\text{F1 score} = \frac{2 \times UA \times PA}{UA + PA} \quad (4)$$

242 In addition, following Tsendbazar et al. (2021), we used a stability index based on the user's and producer's
243 accuracy to evaluate the time-series accuracy consistency of the tree cover map product. The stability index
244 used to evaluate tree cover accuracy is expressed as

$$SI_{t1} = \frac{|TC_{t1} - TC_{t1-1}|}{TC_{t1-1}} \times 100 \quad (5)$$

245 where SI_{t1} is the stability index that indicates the accuracy of tree cover maps (user's or producer's accuracy)
246 at time $t1$, TC_{t1} is tree cover accuracy at time $t1$ and TC_{t1-1} is tree cover accuracy at the previous time ($t0$
247 or the reference year). We also used the maximum and average stability index for two consecutive years to
248 assess the stability of our tree cover products over a long period.

249

250 3 Results

251 We employed two approaches to assess the performance of our Planet-NICFI 2016-2021 tree cover map
252 product. Firstly, we estimated the accuracy of our tree cover products for each year to gain insights into their
253 accuracy and consistency, based on the methods developed by Tsendbazar et al. (2021). In addition, we
254 showed example time series tree cover maps and reported the area dynamics change of tree cover maps during
255 2016-2021. Secondly, we compared our tree cover products to widely used global tree cover products at 10
256 m resolution, including FROM-GLC10 in 2017 (Gong et al., 2019), as well as ESA WorldCover 2020 and
257 2021 (Zanaga et al., 2022; Zanaga et al., 2021).

258

Deleted: Then,

Deleted: 1

Deleted: a study

3.1 Assessment of tree cover map product

Deleted: Statistical accuracy a

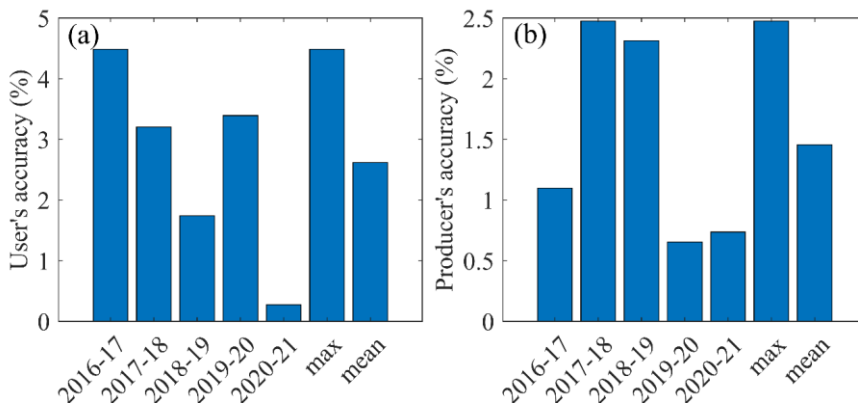
We reported the annual accuracy of the time-series Planet-NICFI tree cover map product in Table 2 with a 95% confidence level. The tree cover accuracy results for 2019 were provided by Yang et al. (2023). The overall accuracy of the tree cover map product ranged between 0.867-0.907 ± 0.015 from 2016 to 2021, with the highest accuracy of 0.907±0.014 in 2021 and the lowest accuracy of 0.867±0.017 in 2016 (Table 2). This discrepancy could be due to poor data in the Planet-NICFI imagery during 2016. The F1 score showed a similar trend from 2016 to 2021, with an average of approximately 0.921. The user's accuracy consistently exceeded 0.901±0.017 over the six years, except for 2016 when it was 0.862±0.021. The producer's accuracies were all higher than 0.912±0.014 (Table 2). Nevertheless, the mapping results of our time-series Planet-NICFI tree cover maps were highly consistent. Additionally, compared to the tree cover, the non-tree cover showed lower user's accuracy, producer's accuracy, and F1 score (i.e., approximately 0.856±0.027, 0.852±0.025, and 0.853, respectively), likely due to the complex composition of non-tree cover types, such as shrubland and herbaceous wetland.

Table 2 User's accuracies, producer's accuracies, F1 score, and overall accuracies of the Planet-NICFI V1.0 2016-2021 tree cover map product for SEA at a 95% confidence level. The accuracy evaluation results in 2019 were provided by Yang et al. (2023).

| Year | Classification | User's accuracy | Producer's accuracy | F1 score | Overall accuracy |
|------|----------------|-----------------|---------------------|----------|------------------|
| 2016 | Tree cover | 0.862±0.021 | 0.925±0.018 | 0.892 | 0.867±0.017 |
| | Non-tree cover | 0.876±0.031 | 0.783±0.026 | 0.827 | |
| 2017 | Tree cover | 0.901±0.017 | 0.935±0.016 | 0.917 | 0.892±0.016 |
| | Non-tree cover | 0.874±0.033 | 0.814±0.027 | 0.843 | |
| 2018 | Tree cover | 0.929±0.016 | 0.912±0.014 | 0.920 | 0.892±0.015 |
| | Non-tree cover | 0.816±0.033 | 0.85±0.030 | 0.832 | |
| 2019 | Tree cover | 0.913±0.012 | 0.933±0.010 | 0.923 | 0.895±0.011 |
| | Non-tree cover | 0.857±0.022 | 0.819±0.021 | 0.837 | |
| 2020 | Tree cover | 0.944±0.014 | 0.927±0.011 | 0.935 | 0.900±0.014 |
| | Non-tree cover | 0.754±0.041 | 0.803±0.040 | 0.778 | |
| 2021 | Tree cover | 0.947±0.014 | 0.934±0.011 | 0.940 | 0.907±0.014 |
| | Non-tree cover | 0.778±0.038 | 0.816±0.039 | 0.796 | |

280

281 We also estimated the stability of our Planet-NICFI tree cover maps accuracy over 2016-2021 (Fig. 3). The
282 results show that the user's and producer's stability indexes were low than 4.5% and 2.5%, respectively,
283 indicating the good stability of our mapped Planet-NICFI tree cover maps for the six years (2016-2021).

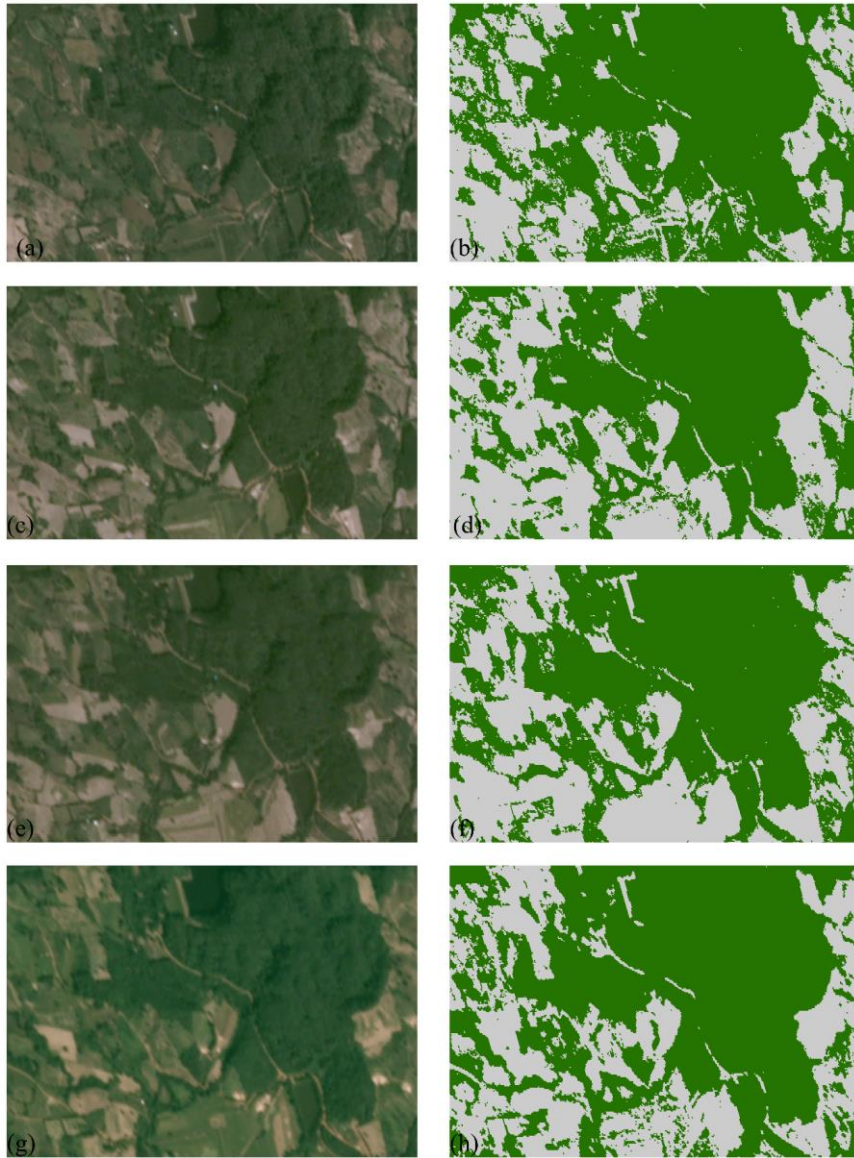


284 **Figure 3** Stability index estimates for the Planet-NICFI tree cover map product 2016-2021: the stability index
285 for (a) the user's accuracy and (b) the producer's accuracy.
286

287

288 We further visually compared our time-series tree cover map product with the original Planet-NICFI imagery
289 during 2016-2019 (Figures 4-5). Note that we have not shown the years 2020 and 2021 due to inconvenient
290 visualization for monthly resolution Planet-NICFI imagery collected from QGIS. In comparison, our tree
291 cover map product showed better consistencies with Planet-NICFI imagery, such as roads, the spatial
292 distribution pattern of tree cover, and non-tree cover. However, our tree cover product potentially exhibited
293 salt and pepper salt and pepper phenomenon in some years (i.e., 2017 and 2018) due to the employment of
294 the RF approach. In practical applications, we need to pay attention to this phenomenon. In addition, we
295 counted the time series of the area estimates of tree cover maps during 2016-2021 and showed a slight
296 increase trend from 2016 to 2021, which is in line with the area estimates of ESA tree cover for the years
297 2020 and 2021. This may be due to forest restoration after the 2015 El Niño phenomenon (Wigneron et al.,

298 [2020](#), as well as the impact of expanded plantations ([Xu et al., 2020](#)).



299 **Figure 4** Time series of the derived tree cover maps for the selected mainland SEA area (100.301°-100.322°E,
300 18.400°-18.409°N). (a) and (b), (c) and (d), (e) and (f), and (g) and (h) indicate 2019, 2018, 2017, and 2017,
301 respectively.
302

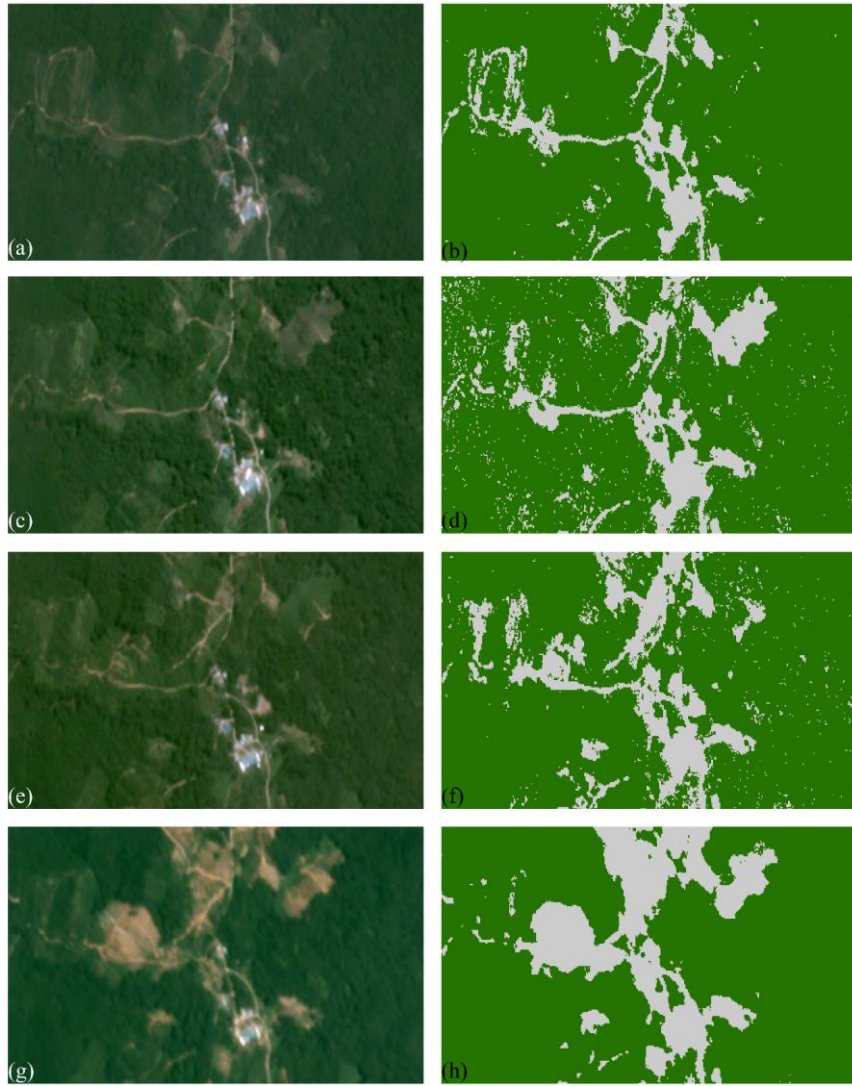


Figure 5 Time series of the derived tree cover maps for the selected maritime SEA area (111.789°-111.806°E, 2.032°-2.040°N). (a) and (b), (c) and (d), (e) and (f), and (g) and (h) indicate 2019, 2018, 2017, and 2017, respectively.

303
304
305
306
307

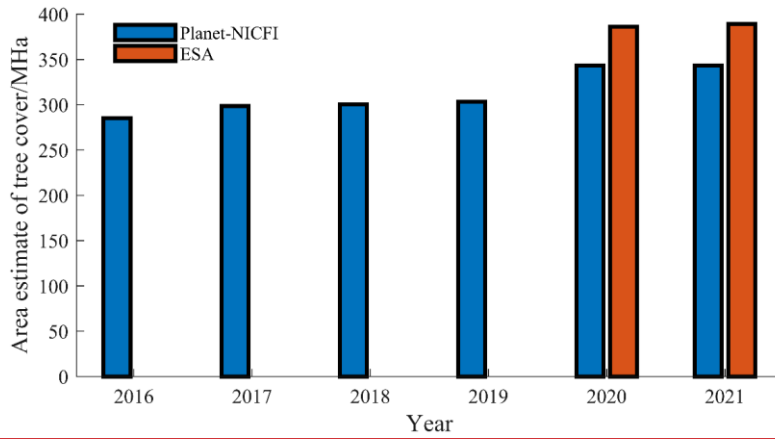


Figure 6 Area dynamics change of tree cover maps for Planet-NICFI and ESA from 2016 to 2021.

3.2 Comparison with existing tree cover products

We compared our mapped Planet-NICFI tree cover maps with FROM-GLC10, ESA WorldCover 2020 and 2021 regarding statistical accuracy (Fig. 4). The results show that our tree cover maps outperformed FROM-GLC10 in user’s accuracy, producer’s accuracy, and overall accuracy. The user’s accuracy and overall accuracy of our tree cover maps exceeded 0.083. ESA WorldCover 2020 and 2021 showed similar performances to our Planet-NICFI tree cover maps. Particularly, the user’s accuracy, producer’s accuracy, and overall accuracy of ESA WorldCover 2020 decreased by 0.020, 0.008, and 0.017, respectively (Fig. 4). This may be because we all used the SAR imagery as input and applied the RF-based machine learning method to classify our tree cover.

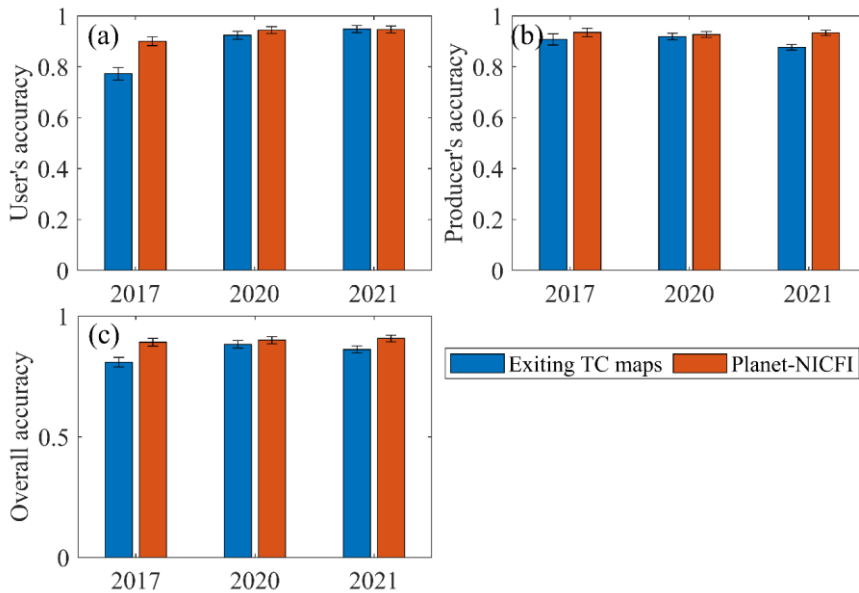


Figure 7 Accuracy comparison between existing tree cover maps and the generated Planet-NICFI tree cover maps at a 95% confidence level: (a) user's accuracy, (b) producer's accuracy, and (c) overall accuracy.

Deleted: 4

We selected six locations (three mainland SEA areas and three maritime SEA areas) to visually compare our Planet-NICFI tree cover maps with three other 10-meter products, namely, FROM-GLC10, ESA WorldCover 2020 and 2021 (Figs. 8-10). In comparison, it is easier for FROM-GLC10 to classify all mixed tree and non-tree areas into non-tree cover maps (Fig. 8a). This may be because FROM-GLC10 cannot apply SAR imagery to tree cover mapping. However, ESA WorldCover 2020 and 2021 can capture tree cover landscapes at a higher level of detail than FROM-GLC, such as long narrow roads, croplands, and built-up areas (Figs. 9-10a). It should be noted that ESA WorldCover 2020 and 2021 omitted some long narrow non-tree cover landscapes and small isolated tree cover and non-tree cover landscapes due to the limitation of the imagery resolution (10 m).

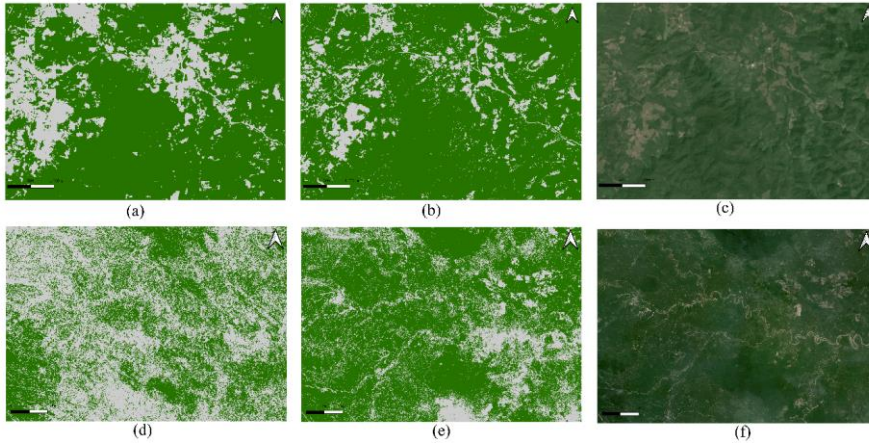
Deleted: 5

Deleted: 7

Deleted: 5a

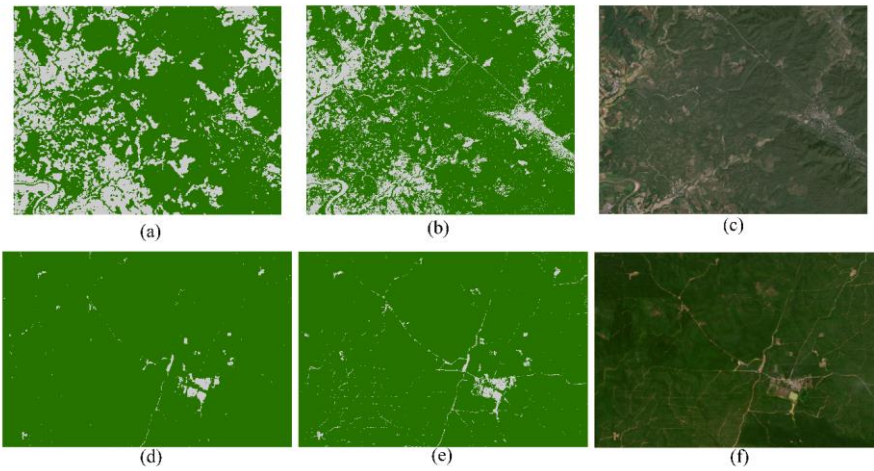
Deleted: 6

Deleted: 7a



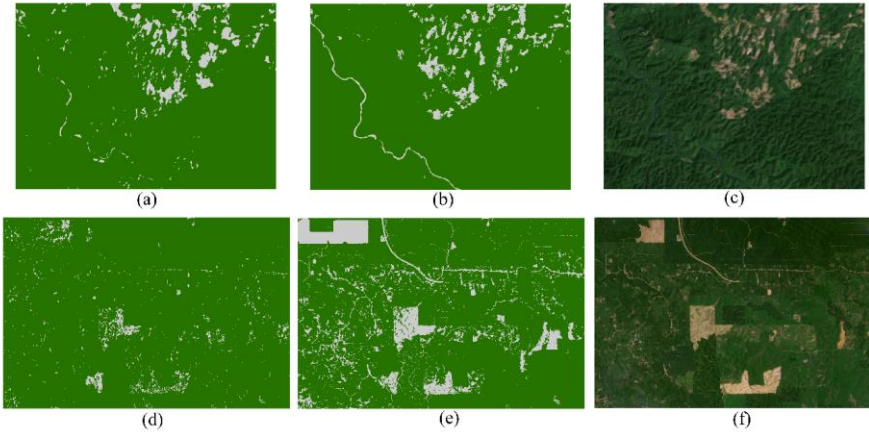
339
 340 **Figure 8** Comparison of FROM-GLC10 (a) and (d), Planet-NICFI tree cover (b) and (e), and Planet-NICFI
 341 imagery (c) and (f) for mainland SEA area (101.594°-101.651°E, 19.254°-19.294°N; top row) and maritime
 342 SEA area (101.925°-103.296°E, -2.096°-1.145°S; bottom row). Green and gray 20% indicate tree cover and
 343 non-tree cover, respectively.
 344

Deleted: 5



345
 346 **Figure 9** Comparison of ESA WorldCover 2020 (a) and (d), Planet-NICFI tree cover (b) and (e), and Planet-
 347 NICFI imagery (c) and (f) for mainland SEA area (98.310°-98.392°E, 17.102°-17.166°N; top row) and
 348 maritime SEA area (99.983°-100.064°E, 1.387°-1.442°N; bottom row). Green and gray 20% indicate tree
 349 cover and non-tree cover, respectively.
 350

Deleted: 6



353
 354 **Figure 10** Comparison of ESA WorldCover 2021 (a) and (d), Planet-NICFI tree cover (b) and (e), and Planet-
 355 NICFI imagery (c) and (f) for Mainland SEA area (102.179°-102.249°E, 18.676°-18.726°N; top row) and
 356 maritime SEA area (99.951°-100.063°E, 1.892°-1.967°E; bottom row). Green and gray 20% indicate tree
 357 cover and non-tree cover, respectively.
 358

Deleted: 7

359 **4 Discussion**

360 Our time-series Planet-NICFI tree cover products were mapped twice a year to mitigate the impact of smog,
 361 light, cloud, and topographic effects in tropical areas (Roy et al., 2021; Marta et al., 2018). These high-
 362 resolution tree cover products meet the minimum tree height requirement of ≥ 5 m [for further generating](#)
 363 [forest data](#). However, it should be noted that we cannot guarantee 100% tree cover for each higher-resolution
 364 pixel, which may introduce some uncertainties when using the higher-resolution tree cover maps. Despite
 365 excluding plantations during sample point labeling, some plantations, such as oil palm, may still be mixed
 366 into our tree cover products due to similarities in anomalies (Mugabowindekwe et al., 2023; Zanaga et al.,
 367 2022; Zanaga et al., 2021). As a result, caution should be exercised when using our Planet-NICFI tree cover
 368 products for certain purposes.

369
 370 To generate [a](#) high-resolution time series tree cover map product at a continental scale, we utilized advanced

372 random forests-based machine learning algorithms on the [GEE](#) platform. However, for fine-scale tree cover
373 mapping, deep learning-based segmentation methods, such as U-net ([Falk et al., 2019](#)), are necessary,
374 particularly when using limited bands (Mugabowindekwe et al., 2023; Wagner et al., 2023; Zanaga et al.,
375 2022; Zanaga et al., 2021; Brandt et al., 2020). As a result, our tree cover map product still has some
376 uncertainty due to limitations in the optical PlanetScope imagery. To improve our tree cover mapping product
377 with higher resolution, we may need to consider adding more bands or utilizing advanced deep learning
378 algorithms in the future.

379

380 **5 Data availability**

381 The high-resolution Planet-NICFI V1.0 time-series tree cover product is now available at
382 <https://cstr.cn/31253.11.sciencedb.07173> (Yang and Zeng, 2023). This product is provided in the Mollweide
383 projection and the World Geodetic System 1984 (WGS1984) datum and geographic coordinate system. Tree
384 cover and non-tree cover are denoted as 0 and 1, respectively, in each yearly file, and are stored as UINT8 in
385 GeoTIFF format. The GeoTIFF files are named Planet-FC_SEA_<YEAR>_prj.tif, for example, Planet-
386 FC_SEA_16_prj.tif.

387

388 **6 Conclusions**

389 We have successfully generated the first accurate and high-resolution time-series tree cover map product for
390 SEA by combining optical and SAR satellite observations, utilizing advanced random forests machine
391 learning algorithms on the GEE platform. Our Planet-NICFI tree cover map product exhibits excellent
392 accuracy and consistency over six years (2016-2021). The baseline tree cover maps, with a resolution of 4.77
393 m, can be easily converted to forest cover maps at different resolutions to cater to the diverse needs of users.

394 Moreover, our tree cover [map](#) product has the unique ability to address rounding errors in forest cover
395 mapping by accurately capturing isolated trees and monitoring the removal of long, narrow forest cover.
396 These cutting-edge fine-scale time-series tree cover maps represent a milestone in forest monitoring and offer
397 unprecedented opportunities for users across diverse disciplines.

398

399 **Code Availability**

400 The scripts used to generate all Planet-NICFI v1.0 tree cover 2016-2021 are provided in JavaScript
401 (https://code.earthengine.google.com/?scriptPath=users%2Fyfhtaurus%2Fcodes%3APlanet_RF-LC_rac).

402 The maps can be automatically generated by running the codes. The scripts are also available on request from
403 Z. Zeng.

404

405 **Acknowledgments**

406 This study was supported by the National Natural Science Foundation of China (grant no. 42071022), the
407 start-up fund provided by the Southern University of Science and Technology (no. 29/Y01296122), and the
408 China Postdoctoral Science Foundation (grant no. 2022M711472). [We thank Sen Jiang, Haowen Duan, Hao](#)
409 [Li, and Fangdong Fu for making tree cover/non-tree cover label data that are used to assess the time series](#)
410 [tree cover map products.](#)

411

412 **Author contributions**

413 Z.Z. designed the research; F.Y. performed the analysis and wrote the draft. All authors contributed to the
414 interpretation of the results and the writing of the paper.

415

416 **Competing interests**

417 The authors declare no competing interests.

418 **References**

- 419 Achard, F., Beuchle, R., Mayaux, P. et al.: Determination of tropical deforestation rates and related carbon
420 losses from 1990 to 2010, *Glob Chang Biol*, 20(8), 2540-2554, 2014.
- 421 Brandt, M., Tucker, C. J., Kariryaa, A., et al.: An unexpectedly large count of trees in the West African Sahara
422 and Sahel, *Nature*, 587(7832), 78-82, 2020.
- 423 Buchhorn, M., Lesiv, M., Tsendbazar, N. E., et al.: Copernicus global land cover layers—collection 2, *Remote
424 Sens.*, 12(6), 1044, 2020.
- 425 Chen, J., Chen, J., Liao, A., et al.: Global land cover mapping at 30 m resolution: A POK-based operational
426 approach. *ISPRS J. Photogramm, Remote Sens.*, 103, 7-27, 2015.
- 427 CoP26, G. L.: Glasgow Leaders' Declaration on Forests and Land Use. Available online at: [https://ukcop26.
428 org/glasgow-leaders-declaration-on-forests-and-land-use/](https://ukcop26.org/glasgow-leaders-declaration-on-forests-and-land-use/)(accessed December 06, 2021).
- 429 ESA: Land Cover CCI Product User Guide Version 2. Tech. Rep. Available at:
430 maps.elie.ucl.ac.be/CCI/viewer/download/ESACCI-LC-Ph2-PUGv2_2.0.pdf, 2017.
- 431 [Falk, T., Mai, D., Bensch, R., et al. U-Net: deep learning for cell counting, detection, and morphometry, *Nat.
432 Methods*, 16\(1\), pp.67-70, 2019.](#)
- 433 FAO: Global forest resources assessment 2020: Main report. Technical report, Food and Agriculture
434 Organization of the United Nations, ROME, 2020.
- 435 Friedl, M., Sulla-Menashe, D.: MCD12Q1 MODIS/Terra+Aqua Land Cover Type Yearly L3 Global 500m
436 SIN Grid V006. NASA EOSDIS Land Processes DAAC. Accessed 2022-12-15 from
437 <https://doi.org/10.5067/MODIS/MCD12Q1.006>, 2019.
- 438 Gong P., Liu H., Zhang M., et al.: Stable classification with limited sample: Transferring a 30-m resolution
439 sample set collected in 2015 to mapping 10-m resolution global land cover in 2017, *Sci. Bull*, 64, 370-
440 373, 2019.
- 441 Gorelick, N., Hancher, M., Dixon, M., et al.: Google Earth Engine: Planetary-scale geospatial analysis for
442 everyone, *Remote Sens. Environ.*, 202, 18-27, 2017.
- 443 Hammer, D., Kraft, R., Wheeler, D.: Alerts of forest disturbance from MODIS imagery, *Int J Appl Earth Obs
444 Geoinf*, 33, 1-9, 2014.
- 445 Hansen, M. C., Potapov, P. V., Moore, R., et al.: High-resolution global maps of 21st-century forest cover
446 change, *Science*, 342(6160), 850-853, 2013.
- 447 Hansen, M. C., Stehman, S. V., Potapov, P. V.: Quantification of global gross forest cover loss, *Proc Natl
448 Acad Sci USA*, 107(19), 8650-8655, 2010.
- 449 Hsieh, P. F., Lee, L. C., Chen, N. Y.: Effect of spatial resolution on classification errors of pure and mixed
450 pixels in remote sensing, *IEEE Trans. Geosci. Remote Sens.*, 39(12), 2657-2663, 2001.
- 451 Karra K., Kontgis C., Statman-Weil Z., et al.: Global land use/land cover with Sentinel 2 and deep learning.
452 In 2021 IEEE international geoscience and remote sensing symposium IGARSS (pp. 4704-4707), IEEE,
453 2021, July.
- 454 Lang, N., Jetz, W., Schindler, K. Wegner, J. D.: A high-resolution canopy height model of the Earth,
455 [doi:10.48550/arxiv.2204.08322](https://doi.org/10.48550/arxiv.2204.08322), 2022.
- 456 Marta, S.: Planet imagery product specifications, Planet Labs: San Francisco, CA, USA, 91, 2018.
- 457 Mugabowindekwe, M., Brandt, M., Chave, J., et al.: Nation-wide mapping of tree-level aboveground carbon
458 stocks in Rwanda, *Nat. Clim. Change*, 1-7, 2023.
- 459 Oishi, Y., Sawada, Y., Kamei, A., et al.: Impact of Changes in Minimum Reflectance on Cloud Discrimination,
460 *Remote Sens.*, 10(5), 693, 2018.

461 Olofsson, P., Foody, G.M., Herold, M., et al.: Good practices for estimating area and assessing accuracy of
462 land change, *Remote Sens. Environ.*, 148, 42-57, 2014.

463 Parker, C., Mitchell, A., Trivedi, M., Mardas, N.: The little REDD book: a guide to governmental and non-
464 governmental proposals for reducing emissions from deforestation and degradation. The little REDD
465 book: a guide to governmental and non-governmental proposals for reducing emissions from
466 deforestation and degradation,
467 http://www.globalcanopy.org/themedia/file/PDFs/LRB_lowres/lrb_en.pdf, 2008.

468 Planet Team: Planet Application Program Interface: In Space for Life on Earth. San Francisco, CA,
469 <https://api.planet.com>, 2017.

470 Reiner, F., Brandt, M., Tong, X., et al.: More than one quarter of Africa's tree cover found outside areas
471 previously classified as forest, 2022.

472 Roy, D.P., Huang, H., Houborg, R., Martins, V.S.: A global analysis of the temporal availability of
473 PlanetScope high spatial resolution multi-spectral imagery, *Remote Sens. Environ.*, 264, 112586, 2021.

474 Sexton, J.O., Noojipady, P., Song, X.P., Feng, M., Song, D.X., Kim, D.H., Anand, A., Huang, C., Channan,
475 S., Pimm, S.L., Townshend, J.R.: Conservation policy and the measurement of forests, *Nat. Clim.*
476 *Change*, 6(2), 192-196, 2016.

477 Shimada, M., Itoh, T., Motooka, T., Watanabe, M., Shiraiishi, T., Thapa, R., & Lucas, R.: New global
478 forest/non-forest maps from ALOS PALSAR data (2007–2010), *Remote Sens. Environ.*, 155, 13-31,
479 2014.

480 Skea J., Shukla P. R., Reisinger A., et al.: Climate change 2022: Mitigation of climate change, IPCC Sixth
481 Assessment Report, 2022.

482 Tsendbazar, N., Herold, M., Li, L., et al.: Towards operational validation of annual global land cover maps,
483 *Remote Sens. Environ.*, 266, 112686, 2021.

484 Velasco, R.F., Lippe, M., Tamayo, F., et al.: Towards accurate mapping of forest in tropical landscapes: A
485 comparison of datasets on how forest transition matters, *Remote Sens. Environ.*, 274, 112997, 2022.

486 Wagner, F. H., Dalagnol, R., Silva-Junior, C. H., et al.: Mapping Tropical Forest Cover and Deforestation
487 with Planet NICFI Satellite Images and Deep Learning in Mato Grosso State (Brazil) from 2015 to 2021,
488 *Remote Sens.*, 15(2), 521, 2023.

489 ~~Wigneron, J.P., Fan, L., Ciais, P., et al. Tropical forests did not recover from the strong 2015–2016 El Niño
490 event. *Sci. Adv.*, 6(6), p.eaay4603, 2020.~~

491 ~~Xu, Y., Yu, L., Li, W., et al. Annual oil palm plantation maps in Malaysia and Indonesia from 2001 to 2016,
492 *Earth Syst. Sci. Data*, 12(2), pp.847-867, 2020.~~

493 ~~Yang, F., Jiang X., Alan D. Ziegler, et al. Improved fine-scale tropical forest cover mapping for Southeast
494 Asia using Planet-NICFI and Sentinel-1 imagery, *J. Remote Sens.*, 2023.~~

495 Feng, Y., Ziegler, A. D., Elsen, P. R. et al.: Upward expansion and acceleration of forest clearance in the
496 mountains of Southeast Asia, *Nat. Sustain*, 4(10), 892-899, 2021.

497 Zanaga D., Van De Kerchove R., Daems D., et al.: ESA WorldCover 10 m 2021 v200,
498 <https://doi.org/10.5281/zenodo.7254221>, 2022.

499 Zanaga D., Van De Kerchove R., De Keersmaecker W., et al.: ESA WorldCover 10 m 2020 v100,
500 <https://doi.org/10.5281/zenodo.5571936>, 2021.

501 Zeng, Z., Estes, L., Ziegler, A. D., et al.: Highland cropland expansion and forest loss in Southeast Asia in
502 the twenty-first century, *Nat. Geosci*, 11(8), 556-562, 2018a.

503 Zeng, Z., Gower, D. and Wood, E. F.: Accelerating Forest loss in Southeast Asian Massif in the 21st century:
504 A case study in Nan Province, Thailand, *Glob Chang Biol*, 24, 4682-4695, 2018b.

Deleted: Yang, F., Jiang, X., Ziegler, A. D., et al.: Improved fine-scale tropical forest cover mapping using Planet and Sentinel-1 imagery, Unpublished, 2023